original article

*Diabetes, Obesity and Metabolism* 12: 591–603, 2010.


ORIGINAL ARTICLE

# Additive actions of the cannabinoid and neuropeptide Y systems on adiposity and lipid oxidation

L. Zhang[1], N. J. Lee[1], A. D. Nguyen[1], R. F. Enriquez[2], S. J. Riepler[1], B. Stehrer[1], E. Yulyaningsih[1], S. Lin[1], Y. C. Shi[1], P. A. Baldock[2], H. Herzog[1,3,*] & A. Sainsbury[1,4,*]

[1]*Neuroscience Research Program, Garvan Institute of Medical Research, St Vincent's Hospital, Darlinghurst, Sydney, NSW 2010, Australia*
[2]*Bone and Mineral Research Program, Garvan Institute of Medical Research, St Vincent's Hospital, Darlinghurst, Sydney, NSW 2010, Australia*
[3]*Faculty of Medicine, University of NSW, Sydney, NSW, Australia*
[4]*School of Medical Sciences, University of NSW, Sydney, NSW, Australia*

**Aims:** Energy homeostasis is regulated by a complex interaction of molecules and pathways, and new antiobesity treatments are likely to require multiple pharmacological targeting of anorexigenic or orexigenic pathways to achieve effective loss of excess body weight and adiposity. Cannabinoids, acting via the cannabinoid-1 (CB1) receptor, and neuropeptide Y (NPY) are important modulators of feeding behaviour, energy metabolism and body composition. We investigated the interaction of CB1 and NPY in the regulation of energy homeostasis, hypothesizing that dual blockade of CB1 and NPY signalling will induce greater weight and/or fat loss than that induced by single blockade of either system alone.
**Methods:** We studied the effects of the CB1 antagonist Rimonabant on food intake, body weight, body composition, energy metabolism and bone physiology in wild-type (WT) and NPY knockout ($NPY^{-/-}$) mice. Rimonabant was administered orally at 10 mg/kg body weight twice per day for 3 weeks. Oral Rimonabant was delivered voluntarily to mice via a novel method enabling studies to be carried out in the absence of gavage-induced stress.
**Results:** Mice with dual blockade of CB1 and NPY signalling (Rimonabant-treated $NPY^{-/-}$ mice) exhibited greater reductions in body weight and adiposity than mice with single blockade of either system alone (Rimonabant-treated WT or vehicle-treated $NPY^{-/-}$ mice). These changes occurred without loss of lean tissue mass or bone mass. Furthermore, Rimonabant-treated $NPY^{-/-}$ mice showed a lower respiratory exchange ratio than that seen in Rimonabant-treated WT or vehicle-treated $NPY^{-/-}$ mice, suggesting that this additive effect of dual blockade of CB1 and NPY involves promotion of lipid oxidation. On the other hand, energy expenditure and physical activity were comparable amongst all treatment groups. Interestingly, Rimonabant similarly and transiently reduced spontaneous and fasting-induced food intake in WT and $NPY^{-/-}$ mice in the first hour after administration only, suggesting independent regulation of feeding by CB1 and NPY signalling. In contrast, Rimonabant increased serum corticosterone levels in WT mice, but this effect was not seen in $NPY^{-/-}$ mice, indicating that NPY signalling may be required for effects of CB1 on the hypothalamo-pituitary-adrenal axis.
**Conclusions:** Dual blockade of CB1 and NPY signalling leads to additive reductions in body weight and adiposity without concomitant loss of lean body mass or bone mass. An additive increase in lipid oxidation in dual CB1 and NPY blockade may contribute to the effect on adiposity. These findings open new avenues for more effective treatment of obesity via dual pharmacological manipulations of the CB1 and NPY systems.
**Keywords:** adiposity, bone mass, CB1 receptor, energy homeostasis, NPY

*Date submitted 22 October 2009; date of first decision 25 November 2009; date of final acceptance 26 November 2009*

## Introduction

Obesity, an epidemic disorder and the leading risk factor for type 2 diabetes, results from a prolonged energy imbalance during which intake exceeds expenditure. One of the major obstacles to permanent weight loss in overweight or obese individuals relates to the ability of the body's complex and redundant energy homeostatic systems to defend against loss of body weight and fat mass. Therefore, to develop more effective treatments for obesity, it is important not only to know the identity and functions of individual molecules and pathways involved in the regulation of energy homeostasis but also to understand how these molecules and pathways interact. Among these, endocannabinoids and neuropeptide Y (NPY) are considered to be important modulators of feeding behaviour, energy metabolism and body composition.

Endocannabinoids promote positive energy balance via activation of the cannabinoid-1 (CB1) receptor, which is expressed in peripheral tissues [1–4] as well as in the central nervous system [4,5]. Endocannabinoid/CB1 tone is under the negative control of leptin [6] and is upregulated in obesity at peripheral [2,7] and central [6] sites. Blocking the endogenous cannabinoid system via CB1 antagonism protects against

*Correspondence to:* Prof. Herbert Herzog, Neuroscience Research Program, Garvan Institute of Medical Research, St Vincent's Hospital, 384 Victoria Street, Darlinghurst, Sydney, NSW 2010, Australia.
E-mail: h.herzog@garvan.org.au

*These authors contributed equally to this work.

diet-induced [8–11] and mutation-induced [6,7] obesity in rodents, as well as inducing weight loss and ameliorating metabolic syndromes in humans [12–14]. The antiobesity effects of CB1 antagonism have been ascribed to effects to reduce appetite [4], increase energy expenditure [11,15] and enhance lipid metabolism in adipose tissue [4,16] and liver [1,17].

Whereas CB1 antagonism holds potential as an antiobesity treatment, it is not without possible adverse effects that require further investigation, notably the possibility of reduced bone mass. CB1 receptors expressed on sympathetic nerve terminals [18] negatively regulate the release of noradrenaline [19], which is known to suppress bone formation [20]. Thus, long-term CB1 blockade could conceivably lead to bone loss by alleviating the inhibition on noradrenaline release and thereby enhancing the noradrenaline-induced suppression of bone formation. Indeed, CB1-deficient mice on a C57BL/6J background have a low bone mass phenotype accompanied by increased osteoclast counts and a decreased rate of bone formation [18]. Therefore, to further investigate the role of the CB1 system in the regulation of bone metabolism and to explore the possibility that CB1 antagonism may have adverse effects on bone mass, we examined the effects of 3-week administration of a CB1 antagonist on bone physiology.

While we hypothesize that long-term CB1 blockade may have adverse effects on bone mass, blockade of NPY signalling may improve skeletal health. NPY, via its actions on Y receptors (Y1, Y2, Y4, Y5 and y6), plays a critical role in regulating energy metabolism. Increased central NPY-ergic tonus elicits robust hyperphagia and induces a series of obesogenic changes in association with gain of body weight and fat mass [21–26]. Importantly, when NPY-induced hyperphagia is prevented by pair feeding, central administration of NPY for 5–7 days in rodents leads to significant fat gain without any change in body weight [22,27], showing an important role of NPY in regulating adiposity independently of food intake and body weight. These findings highlight the potential of blocking NPY-ergic pathway in novel antiobesity treatments. In addition to promoting positive energy balance, the NPY-ergic system negatively regulates bone mass [28,29]. Mice lacking Y1 or Y2 receptors show high bone mass, which is attributable to increased bone formation [28,30–33]. In addition, NPY knockout increases while central NPY administration decreases bone mass in mice [29]. Taken together, these data suggest that blocking NPY-ergic signalling may improve skeletal health in addition to having antiobesity benefits.

Interestingly, several lines of evidence suggest a close interaction between the CB1 and NPY pathways in the regulation of energy homeostasis. The massive increase in food intake and body weight observed after acute or chronic hypothalamic NPY administration in wild-type (WT) mice is strongly reduced in $CB1^{-/-}$ mice [34], suggesting that NPY induces at least part of its effects via the CB1 receptor. Conversely, the cannabinoid receptor agonist, anandamide, augments NPY release from rat hypothalamic explants, whereas the CB1 antagonist, AM251, blocks this action [35]. Furthermore, acute administration of the CB1 receptor antagonist Rimonabant significantly reduces NPY mRNA and protein expression in the hypothalamus of food-deprived mice [36]. These studies imply that CB1 blockade may induce at least part of its effects on food intake, body weight and other metabolic parameters via reduction in the secretion of NPY. In conjunction with the opposite effects of the CB1 and NPY systems on bone metabolism, the reported interaction between CB1 and NPY pathways in the control of energy homeostasis highlights the possibility that dual blockade of CB1 and NPY signalling may lead to additive/synergistic loss of body weight and fat mass without adverse effects on bone mass. To test this hypothesis, we investigated the effects of CB1 blockade with Rimonabant with or without NPY blockade by gene deletion on food intake, body weight, energy metabolism, body composition and bone mass in mice. As NPY is an important regulator of stress responses [37], stress induced by gavage, the common means of oral drug delivery, may hinder investigation of interactions between CB1 and NPY pathways. Therefore, we also developed a novel method for voluntary oral administration of Rimonabant to mice.

## Methods

### Animals

All research and animal care procedures were approved by the Garvan Institute/St. Vincent's Hospital Animal Ethics Committee and were in agreement with the Australian Code of Practice for the Care and Use of Animals for Scientific Purpose. Mice were housed under conditions of controlled temperature (22 °C) and illumination (12-h light cycle, lights on at 07:00 h). All mice were fed a normal chow diet (8% calories from fat, 21% calories from protein, 71% calories from carbohydrate, 2.6 kcal/g; Gordon's Speciality Stock Feeds, Yanderra, NSW, Australia) *ad libitum* unless otherwise stated. Details of generation of the germline NPY knockout mice were published previously [38]. All mice were on a mixed C57BL/6-129/SvJ background.

### Voluntary Oral administration of Rimonabant

Rimonabant [*N*-(piperidin-1-yl)-5-(4-chlorophenyl)-1-(2,4-dichlorophenyl)-4-methyl-1H-pyrazole-3-carboxamidehydrochloride] (Sanofi-Aventis, Paris, France) was given to mice orally at 10 mg/kg body weight. To avoid stress induced by gavage, we developed a method to administer Rimonabant voluntarily and orally. This method involves incorporating Rimonabant into artificially flavoured and sweetened jelly and training mice to eat the jelly. The Rimonabant jelly contains 1.26% Rimonabant, 0.1% TWEEN®80 (Sigma-Aldrich, St. Louis, MO, USA), 16% Splenda® (Splenda® Low Calorie Sweetener, Johnson-Johnson Pacific Pty, NSW, Australia), 9.6% gelatine (Davis Gelatin, GELITA Australia Pty, NSW, Australia) and 7.9% flavouring (QUEEN Flavouring Essence Imitation Strawberry, Queen Fine Foods Pty, QLD, Australia). Jelly including all of the above ingredients, except for Rimonabant, was used as a vehicle. The training involves overnight fasting followed by vehicle jelly presentation and 3-day follow-up jelly presentation without food restriction. More than 95% of mice consumed the entire jelly (8 µl/g body weight = 8 $mm^3$/g body weight,

for example, 240 µl for a 30 g mouse = 0.24 $cm^3$) within 5 min of jelly being placed in the cage and maintained this high avidity for jelly over the study period. To evaluate the effectiveness of this voluntary oral administration method, we examined fasting-induced feeding and spontaneous feeding in 10-week-old male WT mice following acute Rimonabant jelly treatment, as Rimonabant is known to transiently reduce food intake [9,39]. Mice in individual cages with paper towel bedding with or without prior 24-h fasting were given either Rimonabant or vehicle jelly at 17:30 hours. Food was given to fasted mice 30 min after jelly consumption. Food intake was determined at 1, 2, 3, 15 and 24 h after representation of food or jelly consumption for measurement of fasting-induced or spontaneous feeding, respectively. Actual food intake was calculated as the weight of pellets taken from the food hopper minus the weight of food spilled in the cage.

## Experimental Protocol

Male WT and $NPY^{-/-}$ mice at 8 weeks of age were transferred from group housing on soft bedding to individual cages with paper towel bedding and allowed to acclimatize for 2 days before being trained to eat the jelly. At 9 weeks of age, basal body weight, body composition including lean mass, fat mass, bone mineral content and bone mineral density measured by dual-energy X-ray absorptiometry (DEXA, as described below) as well as spontaneous food intake (as described above) were determined. Subsequently, mice were separated into groups of equal average body weight, body composition and food intake within each genotype. At 10 weeks of age, the effects of acute Rimonabant treatment on fasting-induced feeding were determined. Thus, mice were fasted from 09:00 hours. At 08:30 hours on the following day, control and treated mice from each genotype received a first dose of vehicle or Rimonabant (10 mg/kg) jelly, respectively. At 09:00 hours, food was given and food intake was determined at 1, 3, 7 and 24 h after refeeding. From 11 weeks of age, treated mice received Rimonabant (10 mg/kg) jelly twice per day at 08:30 and 17:00 hours for 3 weeks, while control mice received vehicle jelly instead. Daily food intake, fecal output and body weight were determined during the first 10 days. Mice were then put back onto soft bedding. During the third week of the treatment period, mice were put in metabolic chambers to determine metabolic rate, respiratory exchange ratio (RER) and physical activity as described below. Mice were injected with 15 mg/kg of the fluorophore calcein (Sigma Chemical, St. Louis, MO, USA) 10 and 3 days before tissue collection to enable subsequent calculation of bone formation rate as described below.

## Tissue Collection

At the end of the 3-week treatment period, *ad libitum* fed animals were culled between 12:00 and 15:00 hours by cervical dislocation followed by decapitation for collection of trunk blood. Serum was stored at −20 °C for subsequent analysis of corticosterone levels as described below. White adipose tissue depots (inguinal, epididymal, retroperitoneal and mesenteric) and brown adipose tissue were removed and weighed. Femurs and tibias were excised, fixed overnight in 4% paraformaldehyde (PFA) in phosphate-buffered saline (PBS) at 4 °C and then stored in 70% ethanol at 4 °C before undergoing micro-computed tomography or histomorphometry as detailed below.

## Serum Corticosterone

Serum corticosterone levels were determined with a radioimmunoassay kit (ICN Biomedicals, Costa Mesa, CA, USA).

## Determination of Metabolic Rate, Respiratory Exchange Ratio and Physical Activity

Metabolic rate was measured by indirect calorimetry using an eight-chamber open-circuit calorimeter (Oxymax Series; Columbus Instruments, Columbus, OH, USA) as described previously [40]. Briefly, preweighed mice were housed individually in specially built Plexiglas cages (20.1 × 10.1 × 12.7 cm). Temperature was maintained at 22 °C with airflow of 0.6 l/min. Food and water were available *ad libitum*. Mice were singly housed for at least 3 days prior to transferring into Plexiglas cages and were acclimatized to the cages for 24 h before recordings commenced. Mice were subsequently monitored in the system for 24 h. Oxygen consumption ($VO_2$) and carbon dioxide production ($VCO_2$) were measured every 27 min. The RER was calculated as the quotient of $VCO_2/VO_2$, with the value of 1 representing 100% carbohydrate oxidation and the value of 0.7 representing 100% fat oxidation [41,42]. Energy expenditure (kcal heat produced) was calculated as calorific value (CV) × $VO_2$, where CV is 3.815 + 1.232 × RER [43]. Data for the 24-h monitoring period were averaged for 1-h intervals for energy expenditure and RER. Ambulatory activity of individually housed mice was evaluated within the metabolic chambers using an OPTO-M3 sensor system (Columbus Instruments), whereby ambulatory counts were a record of consecutive adjacent photobeam breaks. Cumulative ambulatory counts of *X* and *Y* directions were recorded every minute and summed for 1-h intervals.

## Analysis of Body Composition and Bone Densitometry

Upon completion of indirect calorimetry and physical activity measurements, animals were anaesthetized with isoflurane and then scanned using DEXA (Lunar PIXImus2 mouse densitometer; GE Healthcare, Waukesha, WI, USA) to determine whole body lean mass, fat mass, bone mineral content and bone mineral density. The head and the tail were excluded from the analysis of body composition. Whole femoral bone mineral content and bone mineral density were measured using DEXA in excised left hindlimbs. Femurs were scanned with tibiae attached and the knee joint in flexion to 90°, in order to ensure consistent placement and scanning of the sagittal profile.

## Bone Micro-Computed Tomography

Following fixation, left femora were cleaned of muscle and analysed using micro-computed tomography (micro-CT) with a Skyscan 1174 scanner and associated analysis software (Skyscan, Aartselaar, Belgium). During scanning, the femora

were enclosed in a rigid plastic tube filled with 70% ethanol and prevented from moving by polystyrene packing. The X-ray source was set at 50 kV and 800 μA. Scanning was carried out with a 0.5-mm aluminium filter in place to reduce noise and sharpening was set to 40%. Image projections were acquired over an angular range of 180° (angular step of 0.4°), with pixel size of 7.2 μm and the exposure set to 3600 ms. The image slices were reconstructed using NRecon (Skyscan's volumetric reconstruction software), which uses a modified Feldkamp algorithm. Reconstruction was carried out with automated misalignment compensation for each individual sample and the following settings for the whole study samples: beam-hardening correction set to 30%, ring artifact correction set to 5, smoothing set to 4 and the threshold for defect pixel masking set to 10%. The reconstructed images were then straightened using Dataviewer software (Skyscan) and analyses of the cortical bone were carried out in 150 slices (1.07 mm) of selected 750 slices (5.37 mm) proximally from the distal growth plate using CT-Analyser software (Skyscan). Thresholding was applied to the images to segment the bone from the background and the same threshold setting was used for all the samples. The following two-dimensional parameters were measured: total tissue area, bone area, total tissue perimeter, bone perimeter and polar moment of inertia (a basic strength index). Marrow area was manually calculated from these values as tissue area less bone area. Bone perimeter is equivalent to periosteal perimeter, whilst total tissue perimeter is equivalent to periosteal plus endosteal perimeter. Thus, endosteal perimeter was manually calculated as total tissue perimeter less bone perimeter. In addition, three-dimensional analysis generated cortical thickness measurements.

### Bone Histomorphometry

Right femora were bisected transversely at the midpoint of the long axis and the distal half embedded undecalcified in methacrylate resin (Medim-Medizinische Diagnostik, Giessen, Germany) and 5-μm sagittal sections were analysed, as previously described [44]. Briefly, sections were stained for mineralized bone and trabecular bone volume and thickness, and trabecular numbers were calculated. Bone formation (mineralizing surface), mineral apposition rate and bone formation rate were calculated as previously described [44] using fluorescence microscopy (Leica, Heerbrugg, Switzerland).

### Statistical Analyses

All data are expressed as means ± s.e.m. RER and physical activity over the continuous 24-h period were averaged for the whole 24-h period, as well as for the light and dark periods. Differences between knockout and WT mice were assessed by analysis of variance (ANOVA) or repeated-measures ANOVA. Comparisons of energy expenditure (kcal/h) were carried out by analysis of covariance (ANCOVA), with lean body mass and fat mass as the covariates. The adjusted means of energy expenditure at a common lean mass and fat mass for the comparison were generated by ANCOVA. Correlations between measures of adipose tissue mass and RER were determined using linear regression analysis. Statistical analyses were performed with SPSS for Mac OS X, version 16.0.1 (SPSS, Chicago, IL, USA). Statistical significance was defined as $p < 0.05$.

## Results

### Transient Reduction in Food Intake by CB1 Receptor Antagonism in WT and NPY$^{-/-}$ Mice

To examine the effectiveness of the new method to voluntarily and orally deliver Rimonabant, and since Rimonabant has been reported to reduce feeding [9,39], we studied the acute effects of Rimonabant on 24-h fasting-induced food intake and spontaneous food intake in WT mice. As rodents eat mostly during the dark period, Rimonabant was given to mice in this set of studies at 90 min before the commencement of the dark phase followed by multiple measurements into the dark period to examine food intake in the most physiological relevant condition. In 24-h fasted and non-fasted mice, acute treatment of Rimonabant significantly reduced the refeeding and spontaneous food intake during the first hour (table 1), showing the effectiveness of the voluntary oral Rimonabant administration. The suppressive effect of Rimonabant on feeding was transient, however, as food intake determined during 1−2, 2−3, 3−15, 15−24 and 0−24 h was comparable between vehicle-treated and Rimonabant-treated groups (table 1). The accumulated food intake during the entire 24-h refeeding period was also comparable between control and treatment groups (table 1). Taken together, these data show the effective delivery of Rimonabant via the new administration method and highlight a potent, but transient, effect of Rimonabant to suppress feeding in WT mice.

To investigate the possible interactions of CB1 and NPY signalling in feeding regulation, we subsequently examined the acute effect of Rimonabant on 24-h fasting-induced food intake in WT and NPY$^{-/-}$ mice. Rimonabant treatment significantly and transiently reduced fasting-induced feeding in WT and NPY$^{-/-}$ mice alike, with no effect of NPY deletion on food

**Table 1.** Acute effects of oral Rimonabant (10 mg/kg body weight) given 90 min before onset of the dark phase on 24-h fasting-induced food intake and spontaneous food intake in wild-type mice.

| | Vehicle | Rimonabant |
|---|---|---|
| Fasting-induced food intake (g) | | |
| 0 − 1 h | 0.87 ± 0.11 | 0.41 ± 0.07* |
| 1 − 2 h | 0.30 ± 0.07 | 0.30 ± 0.7 |
| 2 − 3 h | 0.36 ± 0.04 | 0.53 ± 0.10 |
| 3 − 15 h | 2.82 ± 0.27 | 3.08 ± 0.43 |
| 15 − 24 h | 1.17 ± 0.25 | 1.41 ± 0.16 |
| 0 − 24 h | 5.51 ± 0.58 | 5.723 ± 0.49 |
| Spontaneous food intake (g) | | |
| 0 − 1 h | 0.30 ± 0.06 | 0.09 ± 0.04* |
| 1 − 2 h | 0.21 ± 0.04 | 0.10 ± 0.04 (p = 0.06) |
| 2 − 3 h | 0.57 ± 0.14 | 0.48 ± 0.12 |
| 3 − 15 h | 2.17 ± 0.29 | 2.30 ± 0.33 |
| 15 − 24 h | 0.49 ± 0.08 | 0.40 ± 0.15 |
| 0 − 24 h | 3.73 ± 0.41 | 3.36 ± 0.38 |

Data are means ± s.e.m. of 7 − 9 mice per group.
*$p < 0.05$ vs. vehicle group.

intake (figure 1A). These data suggest that CB1 may regulate feeding independently of NPY, consistent with a previous report [34].

We further investigated the chronic effect of Rimonabant on daily food intake over a 10-day treatment period with vehicle-treated animals as control. WT and NPY$^{-/-}$ mice had comparable daily food intake (figure 1B, C). Furthermore, chronic treatment with Rimonabant over 10 days had no effects on daily food intake in either WT or NPY$^{-/-}$ mice (figure 1B, C), consistent with the transient action of Rimonabant on feeding (table 1; figure 1A). In addition, daily fecal output over the 10-day treatment period was comparable between WT and NPY$^{-/-}$ mice, and the addition of Rimonabant administration had no effect on daily fecal output in either genotype (figure 1D, E), suggesting blocking CB1 or/and NPY signalling does not alter gastrointestinal absorption.

## Greatest Reduction in Body Weight in Mice is Seen with Dual Blockade of CB1 and NPY Signalling

WT and NPY$^{-/-}$ mice had similar basal body weight (26.1 $\pm$ 0.8 g and 26.7 $\pm$ 0.5 g for WT and NPY$^{-/-}$ mice, respectively, data are means $\pm$ s.e.m. of 6–13 mice per group, NS). During the first 10-day treatment period, Rimonabant treatment lead to reduced body weight gain in both WT and NPY$^{-/-}$ mice, significantly so in WT (figure 1F). Furthermore, NPY deletion alone resulted in markedly attenuated weight gain and Rimonabant-treated NPY$^{-/-}$ mice exhibited the greatest reduction in weight gain among all treatment groups (figure 1F). A similar pattern of changes in body weight gain was seen at the end of 3-week treatment period (figure 1G). These data suggest an additive effect of dual blockade of CB1 and NPY signalling on body weight reduction.

## Greatest Reduction in Adiposity in Mice is Seen with Dual Blockade of CB1 and NPY Signalling

To investigate the effects of CB1 antagonism and NPY ablation on adiposity, we examined whole body fat mass by DEXA scan (figure 2A) and weights of individual white adipose depots (namely inguinal, epididymal, mesenteric and retroperitoneal depots and the summed weights of these depots) (figure 2B–F) by tissue dissection. Rimonabant-treated WT mice had lower adiposity than vehicle-treated WT mice for all measures, except mesenteric white adipose tissue, although this did not reach statistical significance (figure 2A–F). NPY$^{-/-}$ mice exhibited a markedly lean phenotype evidenced in the significantly reduced fat mass in vehicle-treated NPY$^{-/-}$ vs. vehicle-treated WT mice (figure 2A–F), showing a strong reducing effect of NPY ablation on fat storage. It is interesting to note that the decrease in adiposity was greater in vehicle-treated NPY$^{-/-}$ group than Rimonabant-treated WT group, suggesting NPY signalling may exert a greater control on adiposity than CB1 signalling. Most importantly, white adipose tissue mass in Rimonabant-treated NPY$^{-/-}$ mice was significantly lower than vehicle- and Rimonabant-treated WT and lower than vehicle-treated NPY$^{-/-}$ mice, albeit this latter comparison was not statistically significant (figure 2A–F). This again shows an additive effect of dual blockade of CB1 and NPY signalling in this case on reducing fat mass.

## Increased Lipid Oxidation via CB1 Antagonism and NPY Ablation

To investigate the mechanisms through which blockade of CB1 and NPY signalling reduces body weight and adiposity, we performed indirect calorimetry to determine energy expenditure and RER (an index of fuel source for oxidation), as well as concurrent measures of physical activity. Energy expenditure showed a clear circadian rhythm in all treatment groups, with higher energy expenditure throughout the dark period (figure 3A). However, there was no difference in energy expenditure during the 24-h, dark or light period, among all treatment groups (figure 3A, B), suggesting CB1 or NPY blockade alone or in combination do not alter energy expenditure. The unaltered energy expenditure was associated with an unchanged overall physical activity among treatment groups (320 $\pm$ 50, 280 $\pm$ 46, 235 $\pm$ 77 and 164 $\pm$ 22 ambulatory counts/hour for vehicle- and Rimonabant-treated WT, and vehicle- and Rimonabant-treated NPY$^{-/-}$ mice, respectively; data are means $\pm$ s.e.m., NS). All treatment groups showed a clear circadian rhythm in RER with a lower RER during the light period (figure 3C), indicating a greater use of lipid as an oxidative fuel during the light phase. Interestingly, Rimonabant-treated WT mice showed a significant reduction in RER over the 24-h period and during the light period (figure 3C, D), suggesting an increased lipid oxidation as the result of blocking CB1 signalling. Furthermore, NPY$^{-/-}$ mice exhibited a marked decrease in RER during the light period compared with WT mice, and this decrease was more pronounced than that seen in Rimonabant-treated WT mice (figure 3C, D), indicating that NPY blockade leads to a greater increase in lipid oxidation than that induced by CB1 blockade. Importantly, the increased lipid oxidation in NPY$^{-/-}$ mice was further enhanced by the addition of Rimonabant treatment, as evidenced by the lower RER in Rimonabant- vs. vehicle-treated NPY$^{-/-}$ mice during the 6 h after the administration of the second dose of Rimonabant, at 2 h before the commencement of the dark phase (figure 3C). Moreover, the increased lipid oxidation by Rimonabant in both WT and NPY$^{-/-}$ mice suggests independent mechanisms through which CB1 and NPY signalling regulate oxidative fuel selection.

As we have seen an additive effect of CB1 antagonism and NPY ablation on adiposity as well as on RER, we performed correlation analyses between adiposity and RER to determine whether the greater reduction in adiposity by dual blockade of CB1 and NPY signalling may be correlated with greater increase in lipid oxidation. In support of our hypothesis, RER over the 24-h period and during the light phase, but not the dark phase, was significantly correlated with whole body percentage fat mass as well as the weight of individual and summed white adipose depots as a percent of body weight, except for mesenteric white adipose depot (table 2). It is interesting to note that such correlation did not exist between RER and the relative weight of brown adipose tissue (table 2), suggesting that the fat-reducing effects of CB1 and NPY signalling blockade are specific for white adipose tissues but not for an adipose tissue that contributes to thermogenesis, and that the increased lipid oxidation could contribute to the reduced adiposity by CB1 and NPY signalling blockade.

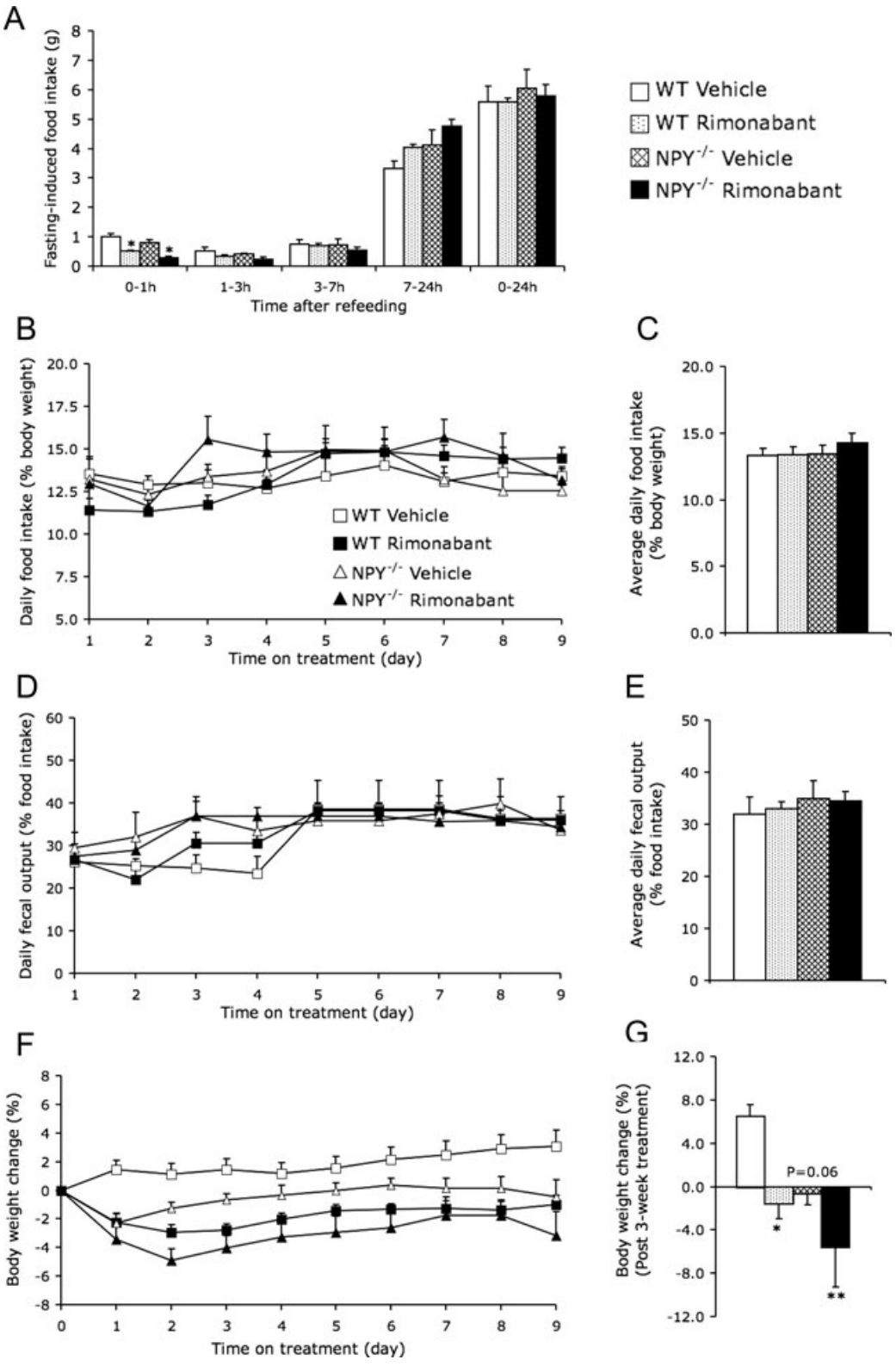


**Figure 1.** Greatest reduction in body weight with transient reduction in food intake in mice seen with dual blockade of cannabinoid-1 (CB1) and neuropeptide Y (NPY) signalling. The 24-h fast-induced food intake in wild-type (WT) and NPY$^{-/-}$ mice after a single oral administration of Rimonabant (10 mg/kg) (A). Daily food intake (B and C), fecal output (D and E) and body weight change (F) during chronic oral Rimonabant treatment (10 mg/kg twice per day) in WT and NPY$^{-/-}$ mice. Body weight change after 3 weeks oral treatment of Rimonabant in WT and NPY$^{-/-}$ mice (G). Data are means ± s.e.m. of 6 − 10 mice per group. *$p < 0.05$, **$p < 0.001$ vs. vehicle-treated WT mice.

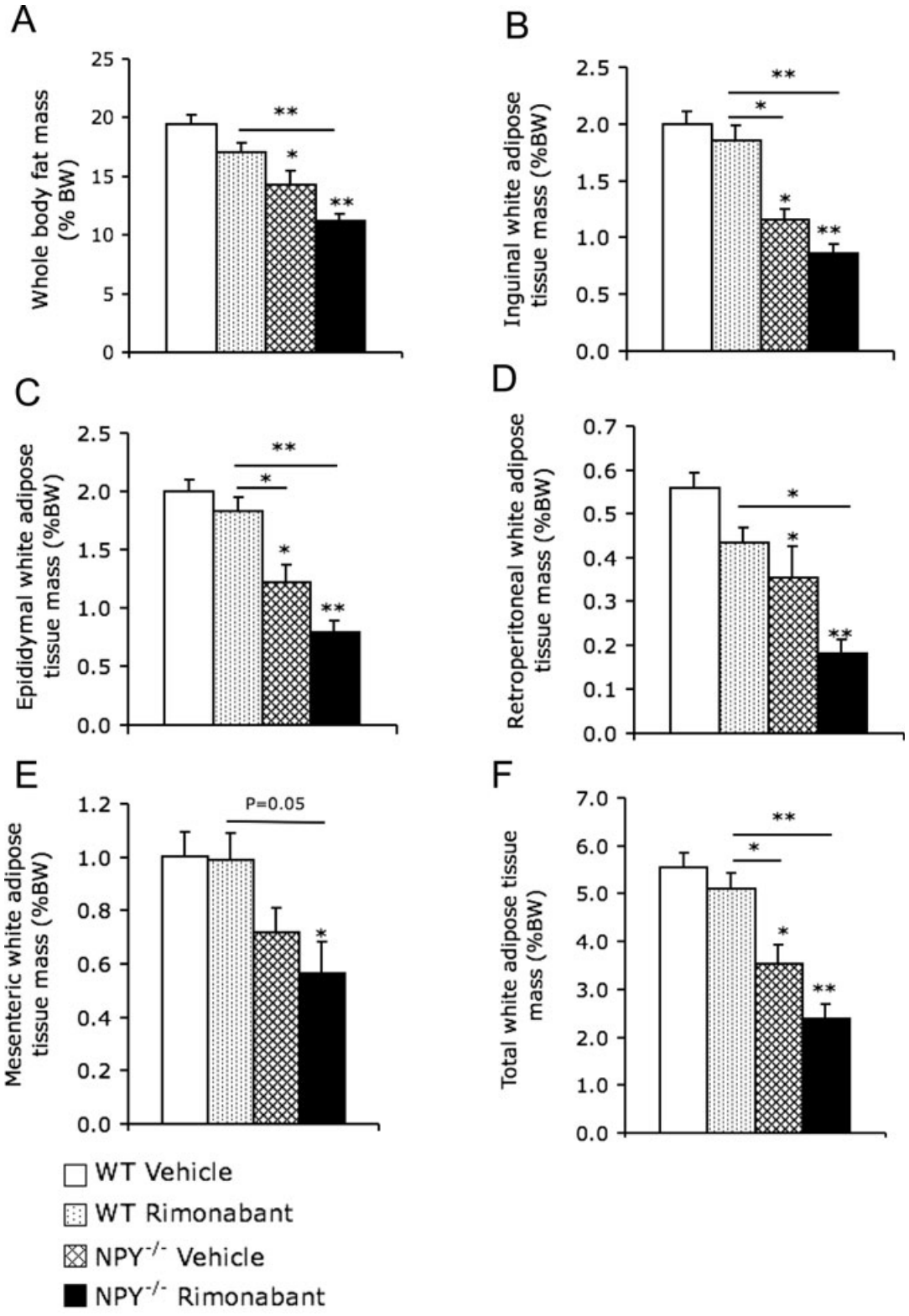


**Figure 2.** Greatest reduction in adiposity in mice seen with dual blockade of cannabinoid-1 (CB1) and neuropeptide Y (NPY) signalling. Whole body fat mass as determined by dual-energy X-ray absorptiometry (DEXA) (A), mass of individual white adipose depots including inguinal (B), epididymal (C), retroperitoneal (D), mesenteric (E) and combined weight of these depots (F) as a percent of body weight (%BW) after 3 weeks of oral Rimonabant treatment (10 mg/kg twice per day) in wild-type (WT) and $NPY^{-/-}$ mice. Data are means ± s.e.m. of 6–10 mice per group. *$p < 0.05$, **$p < 0.001$ vs. vehicle-treated WT mice or the comparison indicated by horizontal bars.

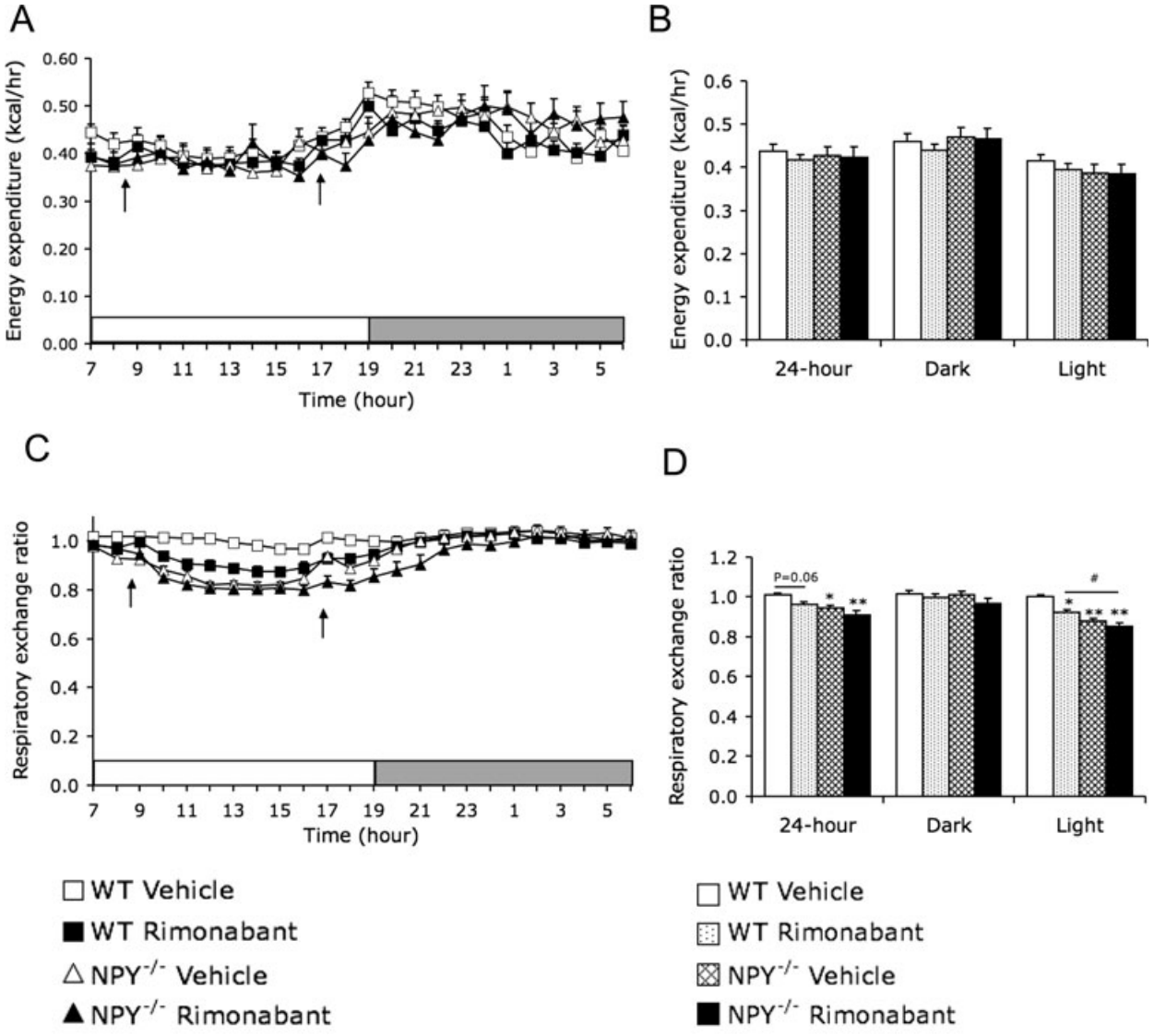


**Figure 3.** Unaltered energy expenditure and increased lipid oxidation in mice with cannabinoid-1 (CB1) and neuropeptide Y (NPY) signalling blockade. Time course of energy expenditure (A) and averages for 24-h, dark and light phases (B), time course of respiratory exchange ratio (C) and averages for 24-h, dark and light phases (D) during chronic oral Rimonabant treatment (10 mg/kg twice per day) in wild-type (WT) and $NPY^{-/-}$ mice. For comparison of energy expenditure by analysis of covariance, common lean mass and fat mass were 19.98 and 4.02 g, respectively. Open and grey horizontal bars and black arrows on (A) and (C) indicate light phase, dark phase and vehicle/Rimonabant administration, respectively. Data are means ± s.e.m. of 6–10 mice per group. *$p < 0.05$, **$p < 0.001$ vs. vehicle-treated WT mice or the comparison indicated by horizontal bars.

**Table 2.** Correlations between respiratory exchange ratio (RER) and adiposity in wild-type (WT) and neuropeptide Y ($NPY^{-/-}$) mice treated orally with Rimonabant or vehicle for 3 weeks.

| | Whole body fat mass (%BW) | WATi (%BW) | WATe (%BW) | WATm (%BW) | WATr (%BW) | WATtotal (%BW) | BAT (%BW) |
|---|---|---|---|---|---|---|---|
| RER 24-h | 0.02 | 0.004 | 0.008 | 0.053 | 0.015 | 0.005 | 0.637 |
| RER light | 0.002 | <0.001 | <0.001 | 0.023 | <0.001 | <0.001 | 0.362 |
| RER dark | 0.4 | 0.240 | 0.379 | 0.263 | 0.5 | 0.234 | 0.852 |

BAT, brown adipose tissue; BW, body weight; WAT, white adipose tissue.
Pearson's correlations were performed between respiratory exchange ratio (RER, during 24-h, light and dark periods) and parameters of adiposity including whole body fat mass as determined by dual-energy X-ray absorptiometry (DEXA) and by the weight of individual white adipose depots as a percentage of body weight (%BW). P values for these correlations are presented. Data were pooled from wild-type and $NPY^{-/-}$ mice with either vehicle or Rimonabant treatment with 6–14 mice per group. WATi, WATe, WATm, WATr and WATtotal indicate inguinal, epididymal, mesenteric, retroperitoneal and the sum of these white adipose tissue depots, respectively.

### No Loss of Lean Body Mass or Bone Mass in Mice with Dual Blockade of CB1 and NPY Signalling

We used DEXA to determine whether the fat-reducing effects of CB1 and NPY signalling blockade are associated with changes in lean body mass and bone mass. Whole body lean tissue mass was comparable between vehicle- and Rimonabant-treated WT mice (figure 4A). Interestingly, NPY$^{-/-}$ mice exhibited a significantly higher percentage of body lean mass compared with WT (figure 4A), which tended to be further enhanced by the addition of Rimonabant treatment (figure 4A). These data suggest that CB1 and NPY signalling blockade specifically reduce fat mass without reducing body lean tissue mass. Moreover, NPY$^{-/-}$ mice showed a trend of higher whole body bone mineral content compared with WT (figure 4B), which was associated with a significantly greater femur length, albeit no significant difference in other bone parameters was observed (table 3). These data suggest that lack of NPY leads to a high bone mass phenotype, consistent with the negative influence of NPY on bone metabolism [28,29]. This is further supported by the fact that Rimonabant-treated NPY$^{-/-}$ mice had a higher bone mass than WT mice (figure 4B). Interestingly, Rimonabant treatment had no effects on all measured bone parameters in either WT or NPY$^{-/-}$ mice (figure 3B; table 3), suggesting that CB1 blockade for 3 weeks does not exert significant effects on bone mass. Taken together, these results show that mice with dual blockade of CB1 and NPY signalling increase or maintain their body lean tissue mass and bone mass, despite significant reductions in adiposity.

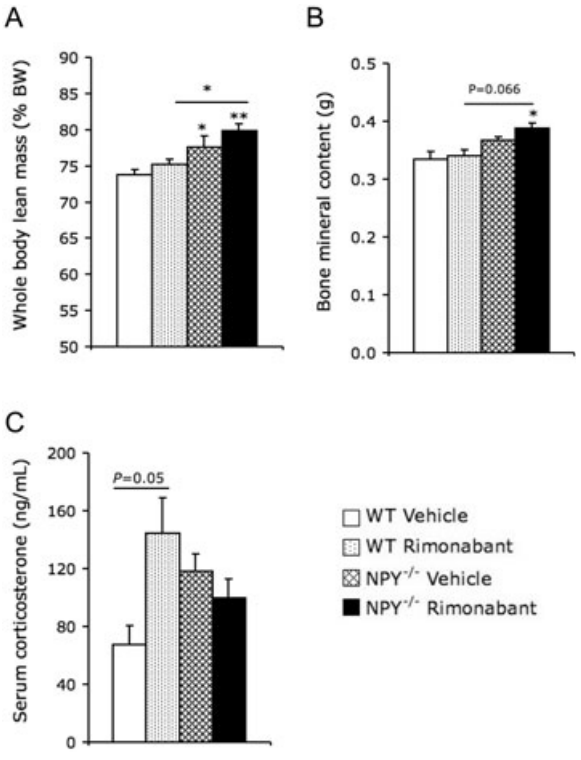


**Figure 4.** Elevated lean body mass and bone mass, but not serum corticosterone levels, in mice with dual blockade of cannabinoid-1 (CB1) and neuropeptide Y (NPY) signalling. Whole body lean mass determined by dual-energy X-ray absorptiometry (DEXA) (A), bone mineral density (B) and serum corticosterone levels (C). Data are means ± s.e.m. of 6–10 mice per group. *$p < 0.05$, **$p < 0.001$ vs. vehicle-treated wild-type (WT) mice or the comparison indicated by horizontal bars.

### Effects of CB1 and NPY Signalling Blockade on Serum Corticosterone Levels

Rimonabant treatment in WT mice significantly increased serum corticosterone levels (figure 4C), suggesting an increased activity of the hypothalamo-pituitary-adrenal (HPA) axis due to CB1 blockade, consistent with previous reports [45,46]. Furthermore, NPY$^{-/-}$ mice showed a trend towards higher serum corticosterone levels compared with WT (figure 4C), consistent with anxiogenic-like phenotype of NPY$^{-/-}$ mice [38] and highlighting the important role of NPY in the control of stress and anxiety. Interestingly, the increase in serum corticosterone by Rimonabant in WT was absent in NPY$^{-/-}$ mice (figure 4C), suggesting that the effect of CB1 on the activity of HPA to increase circulating corticosterone levels may require NPY signalling.

## Discussion

This study shows that dual blockade of CB1 and NPY signalling (as in Rimonabant-treated NPY$^{-/-}$ mice) leads to additive reductions in body weight and adiposity without loss of lean body mass or bone mass. The additive reduction in fat mass is likely because of greater fat oxidation, as mice with dual blockade of CB1 and NPY signalling showed a significant decrease in RER that was more pronounced than that seen in mice with CB1 or NPY blockade alone, and because RER was significantly correlated with adiposity across all groups. Furthermore, whereas CB1 and NPY are both important regulators of energy homeostasis, they appear to regulate feeding and substrate oxidation via independent mechanisms, because Rimonabant transiently reduced feeding and increased lipid oxidation similarly in WT and in NPY$^{-/-}$ mice. In contrast, the effects of CB1 on the HPA axis may require the presence of NPY signalling because the Rimonabant-induced increase in serum corticosterone levels was ablated in NPY$^{-/-}$ mice.

Our study shows a significant reduction in adiposity associated with a significant increase in lipid oxidation in mice with dual blockade of CB1 and NPY signalling, and these changes are greater than those seen in mice with blockade of either CB1 or NPY signalling alone. This suggests a synergistic effect of CB1 and NPY blockade on reducing energy storage at least partially via increased fat oxidation. Indeed, CB1 antagonism induces lipolysis from fat tissue in association with coordinated induction of genes acting at different levels of fatty acid catabolism leading to enhanced $\beta$-oxidation [10,47]. Whereas the effects of CB1 signalling on lipid metabolism appear to occur primarily via peripheral mechanisms [4], actions of NPY signalling on lipid metabolism may involve both central and peripheral mechanisms. Intracerebroventricular administration of NPY, Y1 or Y5 receptor agonists into mice increase RER, suggesting

**Table 3.** Effects of cannabinoid-1 (CB1) and neuropeptide Y (NPY) signalling blockade on bone.

| | WT vehicle | WT Rimonabant | $NPY^{-/-}$ vehicle | $NPY^{-/-}$ Rimonabant |
|---|---|---|---|---|
| Isolated femur length (mm) | 15.06 ± 0.11 | 15.27 ± 0.13 | 16.18 ± 0.04* | 16.22 ± 0.15* |
| Isolated femur mineral content (mg) | 20.00 ± 1.23 | 21.67 ± 0.67 | 22.5 ± 0.76 | 23 ± 0.69 |
| Mineral apposition rate (μm/day) | 1.72 ± 0.09 | 1.59 ± 0.10 | 1.85 ± 0.07 | 1.96 ± 0.10 |
| Total cortical bone tissue area ($mm^2$) | 1.89 ± 0.03 | 1.88 ± 0.10 | 2.03 ± 0.06 | 1.98 ± 0.03 |
| Cortical bone area ($mm^2$) | 0.85 ± 0.02 | 0.83 ± 0.04 | 0.90 ± 0.05 | 0.89 ± 0.02 |
| Bone marrow area ($mm^2$) | 1.05 ± 0.04 | 1.05 ± 0.06 | 1.13 ± 0.03 | 1.10 ± 0.02 |
| Cortical thickness (mm) | 0.20 ± 0.01 | 0.20 ± 0.01 | 0.21 ± 0.01 | 0.21 ± 0.01 |
| Mean polar moment of inertia ($mm^4$) | 0.41 ± 0.01 | 0.41 ± 0.04 | 0.47 ± 0.04 | 0.45 ± 0.01 |

Data are means ± s.e.m. of 3–9 mice per group.
*$p < 0.05$ vs. vehicle-treated wild-type (WT) group.

the involvement of central Y1 and Y5 receptors in the control of substrate oxidation [48]. Furthermore, central activation of Y5 receptors is associated with decreased activity of hormone sensitive lipase (HSL) in mouse adipose tissue, suggesting central-mediated regulation on lipolysis [49]. Peripherally, NPY acts directly on adipocyte-expressed Y1 or Y2 receptors to promote lipolysis in rodents [50,51], dogs [52,53] and humans [52,54,55]. As increased fatty acid availability enhances lipid oxidation [56], enhanced lipolysis via actions of central and/or peripheral perturbations in NPY signalling may be a factor promoting lipid oxidation in $NPY^{-/-}$ mice. Importantly, control of lipid metabolism by peripheral actions of CB1 antagonism may be complemented by effects of lack of NPY signalling at central and peripheral levels. Further studies are required to determine which Y receptor(s) are critical in mediating NPY's effects on fuel selection, and whether pharmacologically blocking the responsible Y receptor(s) recapitulates effects of NPY ablation to enhance fat oxidation and reduce adiposity, particularly in conjunction with simultaneous cannabinoid antagonism. Interestingly, we have recently shown that peripheral Y1 receptors play an important role in regulating substrate oxidation, and mice with reduced Y1 expression in peripheral tissues have enhanced lipid oxidation and are protected from high fat diet-induced obesity [40]. Thus, it would be of interest to investigate the effectiveness of pharmacologically antagonising only peripheral Y1 receptors as a possible antiobesity treatment. Moreover, it should be noted that the CB1 receptor antagonist Rimonabant was withdrawn from the market worldwide in November 2008 due to its psychiatric side-effects, notably increased rates of depression, anxiety and suicide [57]. As our study shows that actions of CB1 antagonism to reduce adiposity are attributable to an increased lipid oxidation, which is primarily mediated via peripheral mechanisms [4], a novel CB1 receptor antagonist that does not act in the central nervous system may be an effective approach to treating obesity without psychiatric side-effects as seen with Rimonabant.

Interestingly, the additive effect of dual CB1 and NPY signalling blockade to reduce adiposity is not because of additive effects on food intake. CB1 blockade by Rimonabant in WT and $NPY^{-/-}$ mice alike leads to reduced fasting-induced and spontaneous food intake. However, these effects were only significant within 1–2 h after administration of Rimonabant, and daily food intake was not altered by acute or chronic administration of Rimonabant. Thus, the effects of CB1 blockade on feeding in WT and $NPY^{-/-}$ mice are unlikely a significant contributor to its effects to reduce body weight and adiposity. This finding suggests the beneficial effects of CB1 blockade on metabolism may exceed its anorexigenic effect, in agreement with previous reports [6–11].

The additive effects of dual CB1 and NPY signalling blockade on adiposity is not because of effects on energy expenditure, as CB1 blockade with Rimonabant for 3 weeks in WT or $NPY^{-/-}$ mice did not enhance energy expenditure. In addition, energy expenditure was not altered in WT mice after a single administration of Rimonabant (data not shown). Studies investigating energy expenditure by indirect calorimetry in rodents show that CB1 blockade increases energy expenditure [10,11,15]. However, this effect has been mostly studied in obese rodent models [11,15], and appears to be transient in that the increase in energy expenditure disappeared in 1 or 12 h after treatment and declines in magnitude with continuous treatment [10,11,15]. Thus, the lack of effects of Rimonabant on energy expenditure seen in this study may be because of the transient effect of CB1 blockade on energy expenditure as well as the unstimulated endocannabinoid/CB1 tone characteristic of lean WT mice [2,6,7].

Our study suggests that NPY signalling may be required for effects of CB1 antagonism on HPA axis activity but not on feeding or substrate oxidation. Recent studies show that acute CB1 blockade reduces NPY release from hypothalamus explants [35] and reduces hypothalamic NPY expression [36], suggesting that the effects of CB1 blockade on energy balance may be mediated via reduction in NPY-ergic tonus, at least acutely. This is likely via indirect mechanisms, because colocalization studies failed to detect CB1 mRNA on NPY-positive neurons in the arcuate nucleus of the hypothalamus [4] or on NPY-positive neurons in key areas of the hypothalamus activated by acute administration of Rimonabant, as determined by induction of c-fos protein [36]. However, our results show that Rimonabant-induced inhibition of spontaneous and fasting-induced feeding remained present in $NPY^{-/-}$ mice, showing that CB1 and NPY signalling regulate appetite independently. Furthermore, CB1 antagonism does not require the NPY system for its effects on lipid oxidation, in keeping with our observation that Rimonabant enhanced lipid oxidation in both WT and $NPY^{-/-}$ mice. In contrast to its effects on food intake and lipid oxidation,

CB1 antagonism appears to require intact NPY signalling for effects on the HPA axis. Indeed, the Rimonabant-induced increase in serum corticosterone levels seen in WT mice—also seen in other studies [45] [46]—was abolished in $NPY^{-/-}$ mice. Taken together, these findings suggest coordinated involvement of the CB1 and NPY systems in the regulation of different parameters that influence energy homeostasis.

It is likely that long-term CB1 antagonism results in compensatory increases in hypothalamic NPY-ergic activity, and this may in turn hinder the effectiveness of CB1 antagonism to reduce adiposity in the longer term. There are reports that although acute CB1 antagonism reduces hypothalamic NPY expression or release [35,36], chronic administration of Rimonabant to rats leads to an upregulation of hypothalamic NPY expression [58]. This may be a compensatory response to the effects of Rimonabant to reduce energy storage and/or it may be secondary to the Rimonabant-induced increase in circulating levels of corticosterone, which is known to stimulate hypothalamic NPY expression [59,60]. Thus, the greater reduction in fat mass induced by blocking NPY signalling, in addition to blocking CB1 with Rimonabant, may be due to prevention of this compensatory increase in central NPY-ergic tonus. This highlights the importance of targeting multiple interacting and compensating pathways involved in regulating energy homeostasis to achieve more effective weight/fat loss.

Finally, our data show that CB1 or NPY signalling blockade, each separately or in combination, reduces adiposity without concomitant loss of lean tissue mass or bone mass. This suggests that pharmacological CB1 blockade has no adverse effect on bone metabolism, but longer studies are required in light of the low bone mass phenotype observed in CB1 knockout mice [18]. In contrast, our data show that lack of NPY signalling promotes a high lean body mass and increased bone mass, likely via central and peripheral actions through Y2 and Y1 receptors, respectively [28,30–33,61]. This finding opens the possibility that dual blockade of CB1 and NPY could protect against possible CB1 antagonist-induced and/or weight loss-induced loss of lean tissue and/or bone during antiobesity treatment.

This study also led us to develop a new, effective and reproducible method of oral and voluntary administration to mice. Thus, animals in this study were investigated in the absence of drug administration-induced stress that is often associated with procedures such as gavage or intraperitoneal injection. This is of particular importance in investigating the biological processes regulated by NPY, as stress is an important modulator of NPY function [37]. Furthermore, this new administration method may prove to be useful in the study of drug pharmacokinetics in experimental animals under more physiologically and clinically relevant conditions.

Taken together, this work showed a coordinated role of CB1 and NPY in the regulation of body composition and energy homeostasis. CB1 and NPY may regulate appetite and fuel oxidation via independent pathways, whereas effects of CB1 signalling on activity of the HPA axis may require the presence of NPY. These coordinated actions lead to greater reductions in body weight and adiposity by dual blockade of NPY and CB1 than that seen after single blockade of either system. Importantly, these effects occur without reducing lean body tissue mass or bone mass and likely involve additive actions of CB1 and NPY blockade to promote lipid oxidation. These findings open new avenues for more effective treatment of obesity via dual pharmacological manipulations of the CB1 and NPY systems. In addition, our novel and effective method for oral and voluntary administration of drug to rodents may prove useful for studies investigating drug pharmacokinetics and effects of oral drug treatment in rodents.

## Acknowledgements

We are grateful to Associate Professor Gregory J. Cooney and Dr Nigel Turner of the Garvan Institute for help with set-up and use of the Columbus Instruments Laboratory Animal Monitoring System. We thank the staff of the Garvan Institute Biological Testing Facility for facilitation of these experiments. This research was supported by a grant from the National Health and Medical Research Council (NHMRC) of Australia and NHMRC Fellowships to H. H. and A. S. This research was supported by an unrestricted grant by Sanofi-Aventis, Australia.

## References

1. Osei-Hyiaman D, DePetrillo M, Pacher P et al. Endocannabinoid activation at hepatic CB1 receptors stimulates fatty acid synthesis and contributes to diet-induced obesity. J Clin Invest 2005; **115:** 1298–1305.
2. Engeli S, Bohnke J, Feldpausch M et al. Activation of the peripheral endocannabinoid system in human obesity. Diabetes 2005; **54:** 2838–2843
3. Cavuoto P, McAinch AJ, Hatzinikolas G, Janovska A, Game P, Wittert GA. The expression of receptors for endocannabinoids in human and rodent skeletal muscle. Biochem Biophys Res Commun 2007; **364:** 105–110.
4. Cota D, Marsicano G, Tschop M et al. The endogenous cannabinoid system affects energy balance via central orexigenic drive and peripheral lipogenesis. J Clin Invest 2003; **112:** 423–431.
5. Herkenham M, Lynn AB, Johnson MR, Melvin LS, de Costa BR, Rice KC. Characterization and localization of cannabinoid receptors in rat brain: a quantitative in vitro autoradiographic study. J Neurosci 1991; **11:** 563–583.
6. Di Marzo V, Goparaju SK, Wang L et al. Leptin-regulated endocannabinoids are involved in maintaining food intake. Nature 2001; **410:** 822–825.
7. Bensaid M, Gary-Bobo M, Esclango A et al. The cannabinoid CB1 receptor antagonist SR141716 increases Acrp30 mRNA expression in adipose tissue of obese fa/fa rats and in cultured adipocyte cells. Mol Pharmacol 2003; **63:** 908–914.
8. Hildebrandt AL, Kelly-Sullivan DM, Black SC. Antiobesity effects of chronic cannabinoid CB1 receptor antagonist treatment in diet-induced obese mice. Eur J Pharmacol 2003; **462:** 125–132.
9. Ravinet-Trillou C, Arnone M, Delgorge C et al. Anti-obesity effect of SR141716, a CB1 receptor antagonist, in diet-induced obese mice. Am J Physiol Regul Integr Comp Physiol 2003; **284:** R345–R353.
10. Herling AW, Gossel M, Haschke G et al. CB1 receptor antagonist AVE1625 affects primarily metabolic parameters independently of reduced food intake in Wistar rats. Am J Physiol Endocrinol Metab 2007; **293:** E826–E832.
11. Herling AW, Kilp S, Elvert R, Haschke G, Kramer W. Increased energy expenditure contributes more to the body weight-reducing effect of rimonabant than reduced food intake in candy-fed wistar rats. Endocrinology 2008; **149:** 2557–2566.

12. Van Gaal LF, Rissanen AM, Scheen AJ, Ziegler O, Rossner S. Effects of the cannabinoid-1 receptor blocker rimonabant on weight reduction and cardiovascular risk factors in overweight patients: 1-year experience from the RIO-Europe study. Lancet 2005; **365:** 1389–1397.

13. Pi-Sunyer FX, Aronne LJ, Heshmati HM, Devin J, Rosenstock J. Effect of rimonabant, a cannabinoid-1 receptor blocker, on weight and cardiometabolic risk factors in overweight or obese patients: RIO-North America: a randomized controlled trial. Jama 2006; **295:** 761–775.

14. Nissen SE, Nicholls SJ, Wolski K et al. Effect of rimonabant on progression of atherosclerosis in patients with abdominal obesity and coronary artery disease: the STRADIVARIUS randomized controlled trial. Jama 2008; **299:** 1547–1560.

15. Liu YL, Connoley IP, Wilson CA, Stock MJ. Effects of the cannabinoid CB1 receptor antagonist SR141716 on oxygen consumption and soleus muscle glucose uptake in Lep(ob)/Lep(ob) mice. Int J Obes (Lond) 2005; **29:** 183–187.

16. Gary-Bobo M, Elachouri G, Scatton B, Le Fur G, Oury-Donat F, Bensaid M. The cannabinoid CB1 receptor antagonist rimonabant (SR141716) inhibits cell proliferation and increases markers of adipocyte maturation in cultured mouse 3T3 F442A preadipocytes. Mol Pharmacol 2006; **69:** 471–478.

17. Osei-Hyiaman D, Liu J, Zhou L et al. Hepatic CB1 receptor is required for development of diet-induced steatosis, dyslipidemia, and insulin and leptin resistance in mice. J Clin Invest 2008; **118:** 3160–3169.

18. Tam J, Ofek O, Fride E et al. Involvement of neuronal cannabinoid receptor CB1 in regulation of bone mass and bone remodeling. Mol Pharmacol 2006; **70:** 786–792.

19. Tam J, Trembovler V, Di Marzo V et al. The cannabinoid CB1 receptor regulates bone formation by modulating adrenergic signaling. Faseb J 2008; **22:** 285–294.

20. Takeda S, Elefteriou F, Levasseur R et al. Leptin regulates bone formation via the sympathetic nervous system. Cell 2002; **111:** 305–317.

21. Raposinho PD, Pierroz DD, Broqua P, White RB, Pedrazzini T, Aubert ML. Chronic administration of neuropeptide Y into the lateral ventricle of C57BL/6J male mice produces an obesity syndrome including hyperphagia, hyperleptinemia, insulin resistance, and hypogonadism. Mol Cell Endocrinol 2001; **185:** 195–204.

22. Sainsbury A, Rohner-Jeanrenaud F, Cusin I et al. Chronic central neuropeptide Y infusion in normal rats: status of the hypothalamo-pituitary-adrenal axis, and vagal mediation of hyperinsulinaemia. Diabetologia 1997; **40:** 1269–1277.

23. Lin EJ, Sainsbury A, Lee NJ et al. Combined deletion of Y1, Y2 and Y4 receptors prevents hypothalamic NPY overexpression-induced hyperinsulinemia despite persistence of hyperphagia and obesity. Endocrinology 2006; **147:** 5094–5101.

24. Kotz CM, Briggs JE, Grace MK, Levine AS, Billington CJ. Divergence of the feeding and thermogenic pathways influenced by NPY in the hypothalamic PVN of the rat. Am J Physiol 1998; **275:** R471–R477.

25. Hwa JJ, Witten MB, Williams P et al. Activation of the NPY Y5 receptor regulates both feeding and energy expenditure. Am J Physiol 1999; **277:** R1428–R1434.

26. Stanley BG, Kyrkouli SE, Lampert S, Leibowitz SF. Neuropeptide Y chronically injected into the hypothalamus: a powerful neurochemical inducer of hyperphagia and obesity. Peptides 1986; **7:** 1189–1192.

27. Zarjevski N, Cusin I, Vettor R, Rohner-Jeanrenaud F, Jeanrenaud B. Chronic intracerebroventricular neuropeptide-Y administration to normal rats mimics hormonal and metabolic changes of obesity. Endocrinology 1993; **133:** 1753–1758.

28. Allison SJ, Baldock PA, Enriquez RF et al. Critical interplay between neuropeptide Y and sex steroid pathways in bone and adipose tissue homeostasis. J Bone Miner Res 2009; **24:** 294–304.

29. Baldock P, Lee NJ, Driessler F et al. Neuropeptide Y knockout mice reveal a central role of NPY in the coordination of bone mass to bone weight. PLoSOne 2009; **4:** e8415.

30. Lundberg P, Allison SJ, Lee NJ et al. Greater bone formation of Y2 knockout mice is associated with increased osteoprogenitor numbers and altered Y1-receptor expression. J Biol Chem 2007; **282:** 19082–91.

31. Baldock PA, Allison SJ, Lundberg P et al. Novel role of Y1 receptors in the coordinated regulation of bone and energy homeostasis. J Biol Chem 2007; **282:** 19092–101.

32. Allison SJ, Baldock P, Sainsbury A et al. Conditional deletion of hypothalamic Y2 receptors reverts gonadectomy-induced bone loss in adult mice. J Biol Chem 2006; **281:** 23436–44.

33. Baldock PA, Sainsbury A, Couzens M et al. Hypothalamic Y2 receptors regulate bone formation. J Clin Invest 2002; **109:** 915–921.

34. Poncelet M, Maruani J, Calassi R, Soubrie P. Overeating, alcohol and sucrose consumption decrease in CB1 receptor deleted mice. Neurosci Lett 2003; **343:** 216–218.

35. Gamber KM, Macarther H, Westfall TC. Cannabinoids augment the release of neuropeptide Y in the rat hypothalamus. Neuropharmacology. 2005; **49:** 646–652.

36. Verty AN, Boon WM, Mallet PE, McGregor IS, Oldfield BJ. Involvement of hypothalamic peptides in the anorectic action of the CB(1) receptor antagonist rimonabant (SR 141716). Eur J Neurosci 2009; **21:** 21.

37. Heilig M. The NPY system in stress, anxiety and depression. Neuropeptides 2004; **38:** 213–224

38. Karl T, Duffy L, Herzog H. Behavioural profile of a new mouse model for NPY deficiency. Eur J Neurosci 2008; **28:** 173–180.

39. Colombo G, Agabio R, Diaz G, Lobina C, Reali R, Gessa GL. Appetite suppression and weight loss after the cannabinoid antagonist SR 141716. Life Sci 1998; **63:** PL113–PL117.

40. Zhang L, Macia L, Turner N et al. Peripheral neuropeptide Y Y1 receptors regulate lipid oxidation and fat accretion. Int J Obes (Lond) 2009; **17:** 17.

41. Ferrannini E. The theoretical bases of indirect calorimetry: a review. Metabolism 1988; **37:** 287–301.

42. Frayn KN. Calculation of substrate oxidation rates in vivo from gaseous exchange. J Appl Physiol 1983; **55:** 628–634.

43. McLean JA, Tobin G. Animal and Human Calorimetry. New York: Cambridge University Press, 1987.

44. Baldock PA, Sainsbury A, Allison S et al. Hypothalamic control of bone formation: distinct actions of leptin and y2 receptor pathways. J Bone Miner Res 2005; **20:** 1851–1857.

45. Patel S, Roelke CT, Rademacher DJ, Cullinan WE, Hillard CJ. Endocannabinoid signaling negatively modulates stress-induced activation of the hypothalamic-pituitary-adrenal axis. Endocrinology 2004; **145:** 5431–5438.

46. Cota D, Steiner MA, Marsicano G et al. Requirement of cannabinoid receptor type 1 for the basal modulation of hypothalamic-pituitary-adrenal axis function. Endocrinology 2007; **148:** 1574–1581.

47. Jbilo O, Ravinet-Trillou C, Arnone M et al. The CB1 receptor antagonist rimonabant reverses the diet-induced obesity phenotype through the regulation of lipolysis and energy balance. Faseb J 2005; **19:** 1567–1569.

48. Henry M, Ghibaudi L, Gao J, Hwa JJ. Energy metabolic profile of mice after chronic activation of central NPY Y1, Y2, or Y5 receptors. Obes Res 2005; **13:** 36–47.

49. Mashiko S, Ishihara A, Iwaasa H et al. Characterization of neuropeptide Y (NPY) Y5 receptor-mediated obesity in mice: chronic intracerebroventricular infusion of D-Trp(34)NPY. Endocrinology 2003; **144:** 1793–1801.

50. Labelle M, Boulanger Y, Fournier A, St Pierre S, Savard R. Tissue-specific regulation of fat cell lipolysis by NPY in 6-OHDA-treated rats. Peptides 1997; **18:** 801–808.

51. Bradley RL, Mansfield JP, Maratos-Flier E. Neuropeptides, including neuropeptide Y and melanocortins, mediate lipolysis in murine adipocytes. Obes Res 2005; **13:** 653–661.

52. Valet P, Berlan M, Beauville M, Crampes F, Montastruc JL, Lafontan M. Neuropeptide Y and peptide YY inhibit lipolysis in human and dog fat cells through a pertussis toxin-sensitive G protein. J Clin Invest 1990; **85:** 291–295.

53. Castan I, Valet P, Voisin T, Quideau N, Laburthe M, Lafontan M. Identification and functional studies of a specific peptide YY-preferring receptor in dog adipocytes. Endocrinology 1992; **131:** 1970–1976.

54. Serradeil-Le Gal C, Lafontan M, Raufaste D et al. Characterization of NPY receptors controlling lipolysis and leptin secretion in human adipocytes. FEBS Lett 2000; **475:** 150–156.

55. Castan I, Valet P, Quideau N et al. Antilipolytic effects of alpha 2-adrenergic agonists, neuropeptide Y, adenosine, and PGE1 in mammal adipocytes. Am J Physiol 1994; **266:** R1141–R1147.

56. Turner N, Bruce CR, Beale SM et al. Excess lipid availability increases mitochondrial fatty acid oxidative capacity in muscle: evidence against a role for reduced fatty acid oxidation in lipid-induced insulin resistance in rodents. Diabetes 2007; **56:** 2085–2092.

57. Sanofi-Aventis to Discontinue All Clinical Trials with Rimonabant. Paris: 2008.

58. Doyon C, Denis RG, Baraboi ED et al. Effects of rimonabant (SR141716) on fasting-induced hypothalamic-pituitary-adrenal axis and neuronal activation in lean and obese Zucker rats. Diabetes 2006; **55:** 3403–3410.

59. Konno J, Yoshida S, Ina A et al. Upregulated expression of neuropeptide Y in hypothalamic-pituitary system of rats by chronic dexamethasone administration. Neurosci Res 2008; **60:** 259–265.

60. Shimizu H, Arima H, Watanabe M et al. Glucocorticoids increase neuropeptide Y and agouti-related peptide gene expression via adenosine monophosphate-activated protein kinase signaling in the arcuate nucleus of rats. Endocrinology 2008; **149:** 4544–4553.

61. Sainsbury A, Schwarzer C, Couzens M et al. Important role of hypothalamic Y2 receptors in body weight regulation revealed in conditional knockout mice. Proc Natl Acad Sci U S A 2002; **99:** 8938–8943.